Computers in Biology and Medicine 139 (2021) 104996

Contents lists available at ScienceDirect

Computers in Biology and Medicine

journal homepage: www.elsevier.com/locate/compbiomed

Combination of docetaxel and newly synthesized 9-Br-trimethoxybenzyl--noscapine improve tubulin binding and enhances antitumor activity in breast cancer cells

Shruti Gamya Dash [a], Srinivas Kantevari [b], Santosh Kumar Guru [c], Pradeep Kumar Naik [a,*]

[a] Centre of Excellence in Natural Products and Therapeutics, Department of Biotechnology and Bioinformatics, Sambalpur University, Jyoti Vihar, Burla, Sambalpur, 768 019, Odisha, India
[b] Fluoro and Agrochemicals Division, CSIR-Indian Institute of Chemical Technology, Hyderabad, 500 007, India
[c] Department of Biological Sciences (Pharmacology & Toxicology), National Institute of Pharmaceutical Education and Research. Hyderabad, Telangana, 500 037, India

ARTICLE INFO

Keywords:
Anti-tumour activity
BTN
DOX
Combination drug therapy
Molecular docking
Tubulin binding affinity

ABSTRACT

To strategically design and frame the novel 9-Br-Trimethoxybenzyl noscapine (BTN) with rigorous binding affinity with tubulin, the structure of noscapine (an antitussive plant alkaloid) was amended with a 3,4,5-trimethoxybenzyl group linked at the seventh position on the lower isobenzofuran unit. Molecular modelling and cellular studies were used to assess the single and combined effects of BTN and docetaxel (DOX). Based on MM-GBSA, the individual calculated free energies of binding ($\Delta G_{bind,\ pred}$) for BTN and DOX with tubulin was found to be −25.69 and −38.17 kcal/mol, respectively, and −29.11 and −36.60 kcal/mol based on MM-PBSA. Furthermore, the $\Delta G_{bind,pred}$ of BTN was dramatically reduced (−30.02 and −33.54 kcal/mol using MM-GBSA and MM-PBSA) in presence of DOX on its binding pocket. Parenthetically, the $\Delta G_{bind,pred}$ of DOX was substantially decreased (−39.17 and −35.80 kcal/mol using MM-GBSA and MM-PBSA) in the presence of BTN on its binding pocket. The synergistic activity of both compounds on tubulin dimmer was also analysed using purified tubulin, where a combined regimen of BTN and DOX attenuated tubulin intensity to a higher value (50%) particularly in comparison to the single regimen. In comparison to the single regimen, the combination of BTN and DOX effectively prevents cell cycle progression during the G2/M phase and induces breast cancer cell death. Female athymic nude mice were xenografted with MCF-7 cells and the efficacy of (150 mg/kg/day), DOX (1.5 mg/kg/week, i.v.), or in combination (BTN 300 mg/kg/day + DOX 1.0 mg/kg/week, i.v) were evaluated.

1. Introduction

Noscapine, an opium alkaloid kills tumour cells by targeting microtubules in a delicate manner [1]. It binds to tubulin dimer with a 1:1 stoichiometry, disrupts the tubulin conformation upon binding and prohibits the dividing cells at mitosis [1]. However, the cancer cells selectively undergo apoptosis because of the compromised cell cycle check points, without hampering the normal dividing normal cells. Individual polymerizing MTs *in vitro* were meticulously monitored in real time, as well as plus end growth over time, and it was discovered that noscapine strongly influenced MT-dynamics by raising the amount of time MTs spent in an attenuated pause state, instead of engaging in appropriate depolymerization and repolymerization [2]. Despite the fact that noscapine primarily influences MT dynamics, cellular activities that do not necessitate accurate control of MT dynamics may be unaffected. As a consequence, noscapine has no apparent neurotoxic effect on peripheral nerve histologies [3]. It has favourable pharmacokinetics *in vivo* (clearance within ~10 h) [4] and has no major potential adverse effects in tissues such as bone marrow, spleen, kidney, heart, liver, or small intestine and does not supress primary humoral immune responses in mice [3,5]. Noscapine and its synthetic derivatives have been shown *in vitro* and in mouse xenograft models to be effective in the treatment of tumour cells derived from multiple of cancers, including colon cancer, non-small cell lung cancer, brain cancer, ovarian cancer, kidney cancer, prostate cancer, leukaemia, breast cancer, and bladder cancer [1,5,6]. To add to its anti-tumor activities, Noscapine is a non-narcotic derivative of opium that lacks analgesic, sedative and respiratory-depressant properties and it does not promote euphoria or dependence [7]. These

* Corresponding author.
E-mail address: pknaik1973@gmail.com (P.K. Naik).

https://doi.org/10.1016/j.compbiomed.2021.104996
Received 2 October 2021; Received in revised form 24 October 2021; Accepted 25 October 2021
Available online 29 October 2021

properties enable its therapeutic use at high concentrations (~150–300 mg/kg body weight) in murine models of human cancer [3,6]. It has been demonstrated that it is effective in attenuating proliferation and designed to induce apoptosis in human ovarian cancer cell lines that are susceptible or resistant to paclitaxel [2]. Noscapine's oral bioavailability provides additional support for its clinical progress as a novel anticancer agent [8].

In the clinic, it has been used as orally available, safe antitussive drug for over 40 years. The harmless effect of noscapine and its derivatives (noscapinoids) on normal tissues is one of the important clinical parameters [9]. Although several synthesized derivatives of noscapine showed promising *in vitro* activities against tumour cell lines, they were unable to achieve complete elimination of the disease despite increased dosages [9]. As a result, combination therapy emerged as a response, in which the anticancer activity of two drugs targeted to tubulin may added up and improve the therapeutic outcome. As an example, combination of docetaxel and other agents has previously been reported to boost the anti-cancer activity of lung cancer [10–13] as well as breast cancer [14]. The combination drug regimen of docetaxel with noscapine derivatives also offers another advantage to minimize the toxicity of docetaxel with normal healthy cells by decreasing its toxic dose and compensating its activity with increasing concentration of noscapinoids. In this study we have used one of the derivatives of noscapine, 9-Br-Trimethoxybenzyl-Noscapine (Fig. 1a) which exhibited improved anticancer efficacy compared to noscapine [15] and evaluate its combined effect with the clinically approved anticancer agent, docetaxel (Fig. 1b) based on *in vitro* cellular and *in vivo* animal model.

2. Materials and methods

2.1. Biology

2.1.1. Cell lines and chemical

The lead compound noscapine and DOX were originally derived from Sigma. BTN, a noscapine analogue, Scheme 1 was chemically synthesied as stated below [15] and refined by HPLC (purity >82%). The MCF-7 breast cancer cell line (ER-positive and PR-positive) was procured from the NCCS, Pune, Maharashtra, India, and all other standard chemicals, reagents, and media utilised mostly in cell culture were purchased from Mediatech, Cellgro. After receiving the cell line, frozen stocks were formed immediately in early passages and were used in the study. Stock solution of BTN (100 mM) was prepared in dimethyl sulfoxide (DMSO) and kept at −20 °C for until use. The MCF-7 cancer cells were grown in the ATCC-recommended (DMEM, Pan Biotech) supplemented with 10% fetal bovine serum (FBS) and 1% antibiotics. The cell lines were cultured at an optimum condition and favourable temperature of 37 °C, 5% CO_2, and 95% humidity. Cells were sub-cultured at 70–80% confluence with trypsin-EDTA (0.25%) for bioassays.

2.1.2. In vitro cytotoxicity studies

The cell proliferation analysis was performed using the 3-(4, 5-dimethylthiazol-2-yl)-2, 5, ditetrazolium bromide (MTT) assay [16]. Briefly, MCF-7 cells were plated in 96 well microtiter plates at a density of 3×10^3 cells/well. After post attachment of 24 h the cells were treated with the variable concentrations of test compounds, BTN (5, 10, 25 and 50 μM) and DOX (0.001, 0.01, 0.1 and 1 μM) in single and also in their combinations (5 μM BTN +1 μM DOX, 10 μM BTN +0.1 μM DOX, 25 μM BTN + 0.01 μM DOX and 50 μM BTN +0.001 μM DOX) for a duration of 48 h and 72 h. After incubation, 10 μl of MTT (5 mg/ml) was poured to each well and incubated for 4 h, at 37 °C and the absorbance was measured in a plate reader (Varioskan, Thermo Scientific) at 570 nm. The IC_{50} values of the compounds (the drug concentration supposed to kill 50% of the cells) were estimated by using online resource Quest GraphTM IC_{50} analyser (AAT Bioquest, Inc., Sunnyvale, CA, USA, https://www.aatbio.com/tools/ic50-calculator). Further, the combined concentration of BTN and DOX to inhibit 50% of the cellular proliferation of MCF-7 was also determined. The experiments were repeated in triplicates.

2.1.3. Drug combination effect study using isobologram analysis

Isobolographic analysis, a dose-oriented geometric method of evaluating drug interactions, was used to analyse the interactions between BTN and DOX [17]. Due to the non-constant dose ratio of BTN and DOX, a normalized isobologram for the two drugs at their ED50 was automatically generated by CompuSyn ver. 1.0. Briefly, the fractional inhibitory concentration (FIC) of each drug was calculated based on the equation stated below.

$$FIC = \frac{Conc.of\ drug\ in\ combination\ to\ produce\ 50\%\ cell\ kill}{Conc.of\ drug\ alone\ to\ produce\ 50\%\ cell\ kill}$$

According to the previously reported interpretation, the FIC of both BTN and DOX were summed to generate the Sum FIC value [17].

2.1.4. Inhibition of cell cycle assay

The cell cycle inhibition experiment was carried out using BTN (10 μM) and DOX (0.1 μM) in single and in combination regimen (25 μM BTN + 0.01 μM DOX) against MCF-7 cells following the standard protocol described by Dash et al. [17]. The percentage of cells in various phases of the cell cycle was quantified using a flow cytometer (FACS Calibur).

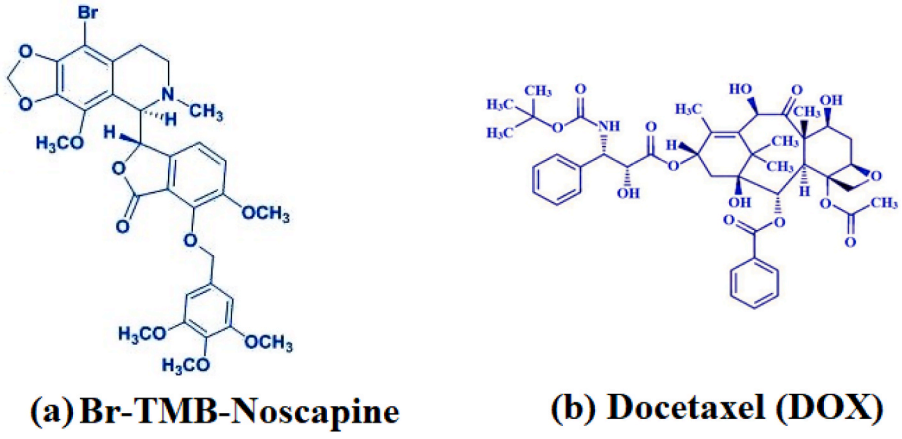

Fig. 1. The molecular structures of (a) rationally designed derivative, Br-TMB-Nos and (b) a clinical tubulin binding anticancer agent, Docetaxel (DOX) used in the study.

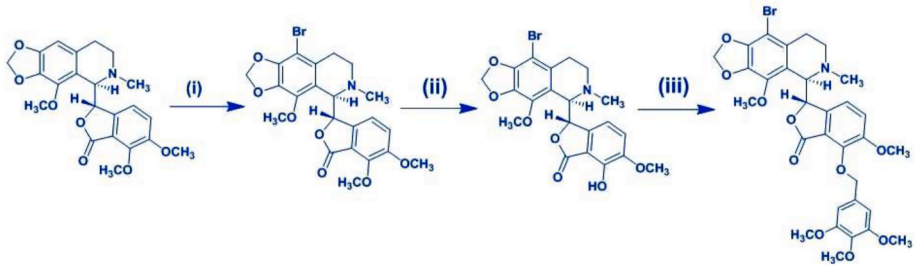

Scheme 1. Synthesis of BTN Reaction Conditions: (i) Br_2–H_2O in 48% Aqueous HBr, 2 h, RT, 90% (ii) NaN_3/NaI, DMF, 4 h, 135–140 °C, 75% (iii) 3,4,5 Trimethoxybenzyl bromide/NaH/TBAI, Toluene: NMP (1:1), 70 °C, 2 h, 82%.

2.1.5. Apoptosis assay

We want to test whether the arrest of cell cycle progression with the treatment of BTN and DOX alone or in their combination regimen, induces apoptosis to cancer cells. The MCF-7 cells (5×10^4) were cultured in 35 mm plates and incubated overnight at a temperature of 37 °C with 5% CO_2. The cells were subsequently treated for up to 24 h with BTN alone (10 μM), DOX alone (0.1 μM), and in their combination regimen (25 μM BTN+0.01 μM DOX). The apoptosis mediated by the BTN and DOX in single or in their combine effect was detected by following the manufacturer's protocol on a flow cytometer (BD FACS Calibur).

2.1.6. DAPI staining

Inverted fluorescence microscopy was used to detect apoptotic cells treated with test drugs after DAPI exposure. MCF-7 cells were cultured on poly-L-lysine coated coverslips in 6-well plates and were treated with BTN (10 μM) alone, DOX (0.1 μM) alone and in their combined concentration (25 μM BTN+0.01 μM DOX) for 48 h. After incubation, coverslips were maintained in cold methanol, rinsed with PBS, labelled with DAPI, and mounted on slides. An inverted fluorescence microscope was used to acquire the images (Nikon Eclipse Ts2R-FL). Changes in morphology were used to distinguish apoptotic cells in comparison to control cells.

2.1.7. Morphological analysis using acridine orange (AO) & ethidium bromide (Etbr) staining

MCF-7 cancer cells were cultured and treated with BTN (10 μM) alone, DOX (0.1 μM) alone or in their combination (25 μM BTN+0.01 μM DOX) BTN and DOX at IC_{50} concentration for 48 h. Coverslips were fixed in cold methanol and then rinsed in PBS after incubation. It was mounted on slides after staining with acridine orange and ethidium bromide. An inverted fluorescence microscope was used to capture images (Nikon Eclipse Ts2R-FL). Apoptosis was detected by distinct variations in morphology relative to untreated cells.

2.1.8. Tryptophan quenching assay

Tubulin is auto fluorescent due to the availability of several tryptophan amino acids. As a result, a fluorescence assay was employed to investigate the reducing pattern of tubulin's inherent tryptophan fluorescence with the treatment of BTN and DOX in single or combination regimens to assess their binding affinity with tubulin. In brief, 2 μM of Tubulin was incubated in a water bath with desired concentration of BTN (10 μM, 25 μM), DOX (0.1 μM) and in combination regimen ((DOX 0.01 μM + BTN 25 μM) (DOX 0.001 μM + BTN 50 μM)) in PEM buffer (50 mM Pipes, 3 mM MgSO4, 1 mM EGTA, pH 6.8) for 45 min at 35 °C [16].

2.1.9. BTN and DOX hindered the conformational changes of tubulin

ANS was previously used to determine the conformational changes of tubulin when a ligand bound to it [14–16]. In brief, 2 μM tubulin in PEM buffer was incubated for 45 min at 35 °C with different concentrations of BTN (10 μM and 25 μM), DOX (0.1 μM) or in their combination regimen (DOX 0.01 μM + BTN 25 μM, DOX 0.001 μM + BTN 50 μM). After adding ANS (50 μM) the samples were incubated in dark at 25 °C for an additional 15 min. The studies were conducted out twice.

The binding of chemical substances to protein and their impact on the overall secondary structure conformational changes of protein was demonstrated using far-UV circular dichroism spectra [18]. Purified tubulin (5 M) was incubated with BTN at a concentration of 10 μM, DOX at a concentration of (0.1 μM) or in their combination regimen (DOX 0.01 μM + BTN 25 μM) in a 25 mM pipes buffer, pH 7.4 for 45 min at a temperature of 35 °C.

2.1.10. In vivo antitumor effect against MCF-7 breast tumors

All experimental protocols involved in this study were approved by the Institutional Animal Ethics Committee of National Institute of Pharmaceutical Education and Research (NIPER), Hyderabad (1548/PO/Re/2011/CPCSEA) and followed by the guidelines of "Committee for the Purpose of Control and Supervision of Experiments on Animals" of Govt. of India. About 8–10 weeks old female BALB/c athymic nude mice were housed in the Animal Care Facility. Suspensions of 1×10^6 human epithelial breast adenocarcinoma MCF-7 cells in 0.2 ml of PBS were inoculated subcutaneously into the anterior flank. After 7–10 days when the tumors were palpable treatment of the test compounds were administrated by oral gavage. The mice were randomly divided into 4 groups. Group-1 (control) consisted of 5 animals which received daily gavage of vehicle solution (acidified water, pH 4.0) only, Group-2 consisted of 5 animals were treated with BTN (150 mg/kg/day), Group-3 (5 animals) were treated with DOX (1.5 mg/kg/week, i.v) and Group-4 consisted of 5 animals were treated with combination dose of BTN and DOX (BTN 300 mg/kg/day + DOX 1.0 mg/kg/week, iv). Tumor volumes were estimated on alternate days by measuring tumors in three transverse direction diameters with vernier callipers and calculating their volume as Π/6 (length x width x height) [19]. The control group of mice was euthanized at day 30 owing to their large tumor volumes this served as the endpoint for control animals. Accordingly, this end point was used to evaluate tumor size in untreated mice with those administered with BTN and DOX.

2.1.11. Histopathological and hematological analyses

On day 40, tumor-bearing mice treated with BTN and DOX in a single or combined regimen, as well as untreated tumor-bearing mice, received an overdose (0.2 ml) of 3.5% chloral hydrate, blood was drawn from the heart, and CBC analysis was conducted using a CBC analyzer (CDC Technologies, Oxford, CT). Following that, the animals were perfused with a 3% paraformaldehyde and 2% glutaraldehyde combination in PBS (pH 7.4), and the liver, kidney, spleen, lung, heart, brain, intestines, and tumour were extracted and analysed for histological investigation. Tissues were mounted in paraffin, sectioned, and stained with hematoxylin and eosin. The tissues were observed under the microscope for toxicity evaluation.

2.2. Molecular modeling

2.2.1. Ligand and protein preparation

The ligands, BTN and DOX, were developed using the maestro molecular builder (Schrodinger). Using a macromodel, the energy of the molecular structures was minimized [20,21]. The molecular structures were also geometrically enhanced using Jaguar (Schrödinger), and we incorporated hybrid density functional theory with Becke's three-parameter exchange potential and the Lee-Yang-Parr correlation functional (B3LYP) [22,23] and the 3-21G* basis set [24,25] based on the theory of (B3LYP).

The tubulin-amino noscapine co-crystal structure (PDB ID: 6Y6D, resolution 2.20 Å) [26] was being used for docking studies of BTN and DOX alone or in combination. The structure was developed using the multistep protein preparation wizard (Schrödinger) with the default parameters set up [27].

2.2.2. Molecular docking

The reported noscapinoid, BTN and DOX binding pockets on tubulin were defined using the Glide grid-receptor generation programme with a concentric grid box at the centroid of the binding site. The mass centre of the docked ligand was intended to be confined inside an inner bounding box 14 Å × 14 Å × 14 Å. In addition, an outer grid box with dimensions of 20 Å × 20 Å x 20 Å was designed, inside which all ligand atoms of a valid configuration must be contained. Both BTN and DOX were docked onto αβ-tubulin heterodimer at their respective binding cavity using Glide-XP docking (Schrödinger) [28]. Further, to the complex of BTN and tubulin, the DOX was docked and similarly to the complex of DOX and tubulin, the BTN was docked. A Glide XP scoring algorithm was used to assess the binding interactions of both ligands [29,30].

2.2.3. Molecular dynamics simulation

The docked complexes of (a) BTN with tubulin, (b) DOX with tubulin, (c) both BTN and DOX in association with tubulin, and (d) tubulin alone were used for the simulation model using the previously mentioned parameters, algorithms, and methodology [17,31–35]. During simulations, the non-bonded interaction cut-off was adjusted at 10 Å, electrostatics was evaluated using Particle Mesh Ewald (PME), and bonds were strictly controlled by using the shake algorithm [36–38]. The Langevin thermostat was used to control the temperature of the simulation. Every 20 ps, coordinates for each molecular system were saved.

2.2.4. Post scoring with MM-GBSA and MM-PBSA

The excepted free energy of binding ($\Delta G_{bind,pred}$) of BTN and DOX in their single binding and in co-binding with tubulin was estimated as the ensemble average of the binding free energy of a total of 250 snapshots from the last 5 ns duration of the MD simulation trajectory of their respective molecular systems [17]. To derive $\Delta G_{bind,pred}$ we adopted MM-GBSA and MM-PBSA methods [39].

3. Results

3.1. (A)

3.1.1. BTN inhibits proliferation of breast cancer cells

We assessed the effectiveness of BTN and DOX in inhibiting the proliferation of human breast cancer cell line (MCF-7) both in single and in combination regimens by MTT assay. With the increasing concentration of BTN and DOX both in single and in combination, the antiproliferative activity was found to increase (Fig. 2). The IC_{50} value for BTN was found to be 10.461 μM and 8.266 μM for 48 h and 72 h of treatments. In contrast, the IC_{50} value for DOX was demonstrated to be 0.033 μM and 0.014 μM for 48 h and 72 h of treatments. Furthermore, our investigation showed that the combination dose of BTN (25 μM) and DOX (0.01 μM) revealed a reduction in cell survival of less more than 50% at 48 and 72 h of treatment. Therefore, the dose-dependent cytotoxicity of DOX may be reduced dramatically with the combination dose regimen of BTN.

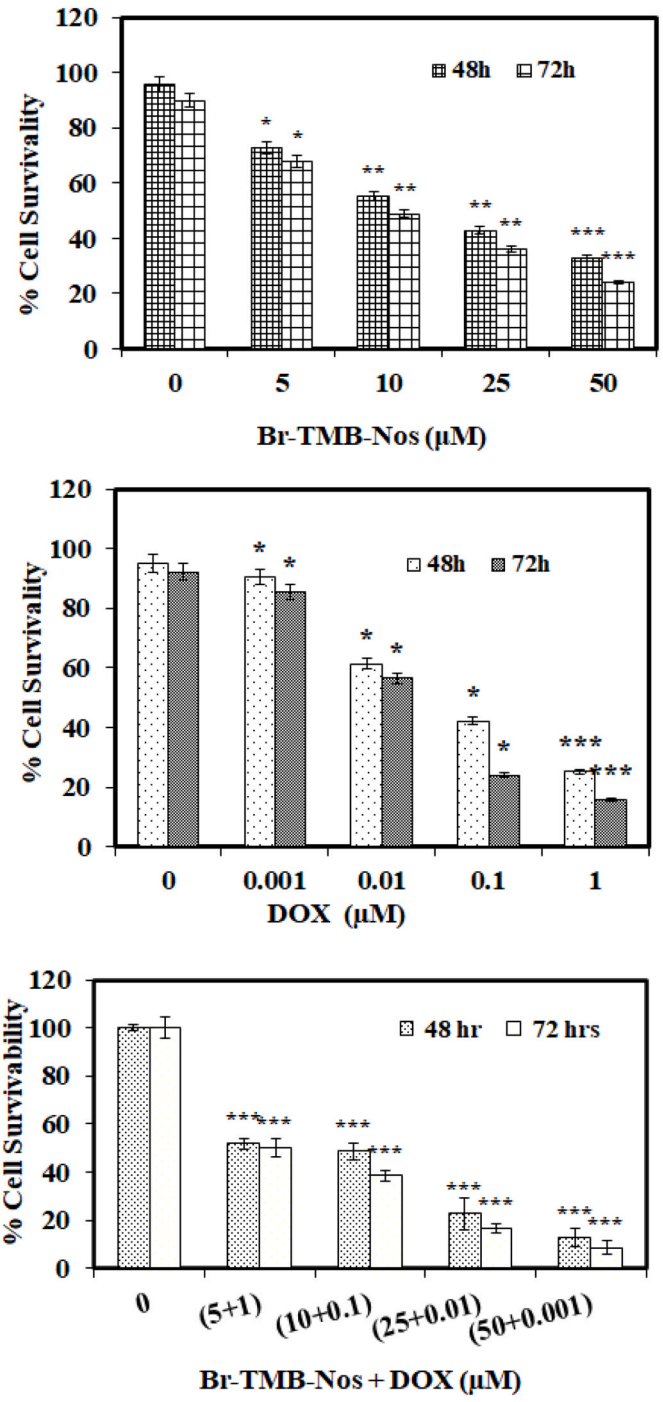

Fig. 2. Br-TMB-Nos and DOX in single as well as in combination regimen at different concentrations inhibit cellular proliferation of human breast cancer cell, MCF-7 after 48 h and 72 h treatment. The IC_{50} value amounted to 10.461 μM and 8.266 μM, respectively for 48 h and 72 h with Br-TMB-Nos Similarly, the IC_{50} value amounted to 0.033 μM and 0.014 μM, respectively for 48 h and 72 h with DOX. In contrast, approximately 50% inhibition of cellular inhibition was achieved in a combination regimen of Br-TMB-Nos (25 μM) and DOX (0.01 μM) after 48 h and 72 h post-treatment. The graph is presented as mean ± SD, (n = 3), and considered significant if *p < 0.05, **p < 0.01, ***p < 0.001 compared to the control.

3.1.2. BTN with DOX exerts synergistic effect against breast cancer cells

To assess the anticancer efficacy of BTN and DOX in combination regimens, MTT assays have been performed to measure the inhibition in the proliferation of MCF-7 cells at different concentrations. The combined effect of BTN and DOX on cell proliferation was evaluated by isobolographic analysis. In MCF-7 cells, the synergistic interaction of the BTN and DOX was observed in the combination of the compounds (Fig. 3). The Sum *FIC* (combination index) values were found to be less than one (0.8 and 0.6 for 48 and 72 h respectively) for 50% cell killing suggesting synergistic interaction of BTN and DOX, rather than additive or antagonistic.

3.1.3. Cell cycle profile and mitotic arrest of cancer cells at G2/M transition level with therapeutic interventions of BTN and DOX

Based on fluorescence-activated cell sorting analysis of drug-treated or untreated MCF-7 cells at 24 h, the efficacy of BTN (10 μM) and DOX (0.1 μM) in single as well as in their combination regimen (25 μM BTN+0.01 μM DOX) on the cell cycle was examined. Untreated cells exposed to vehicle solvent (DMSO) exhibited a typical cell cycle profile, with 63.1% in G1, 5.63% in S, and 29.4% in G2/M. (Fig. 4). Furthermore, after 24 h of treatment with BTN and DOX alone or in combination, there's an increase in sub-G1 cell populations compared to the control. After 24 h treatment the BTN showed only 34.4% in G1 phase, 14.2% in S phase, and 38.7% in G_2/M phase. Parenthetically, treatment with DOX after 24 h revealed 6.86% in G1 phase, 3.33% in S phase and 73.5% in G2/M phase. In contrast, the combination effect of both BTN and DOX after 24 h revealed 23% in G1 phase, 8.23% in S phase and 39.2% in G2/M phase. The sub-G1 population was increased to 12.6% with treatment of BTN, whereas with DOX it was enhanced to 16.4% and in combination, it further increased to 29.6% in comparison to control. Therefore, both the compounds, BTN and DOX alone or in combination showed promising activity in MCF-7 cells which is an event reminiscent of apoptosis to the cancer cell. Maximum percentages of cells were arrested at the G_2/M transition phase.

3.1.4. Induction of apoptotic DNA fragmentation in MCF-7 cells

We next evaluated the induction of apoptosis by BTN and DOX in single or in combination regimen; using 7-Amino-Actinomycin (7-AAD) versus PE-conjugated Annexin V fluorescence staining kit via flow cytometer. The number of apoptotic MCF-7 cells continued to increase following 24 h treatment with BTN (10 μM) and DOX (0.1 μM) alone and in combination regimen (BTN 25 μM + DOX 0.01 μM) in comparison to the control group.

Cells in the first quadrant were necrotic cells, which were Annexin V negative cells. Leading to a shortage of plasma membrane integrity, the second quadrant represents late apoptotic cells that were both Annexin V and 7-AAD positive. The third quadrant includes normal viable cells that were not stained with both Annexin V and 7-AAD. The fourth quadrant comprises early apoptotic cells that were Annexin V positive. In compared to the control group, there was a substantial increase in early and late apoptotic cells following BTN and DOX exposure, both individually and in combination. The percentage of early apoptotic cells measured were 5.33%, 13.5%, 27.8%, and estimated late apoptotic cells were 6.37%, 4.77%, 13.7%, respectively with the treatment of BTN and DOX in single or in combination regimen. The untreated control cells used to have relatively few early and late apoptotic cells (1.16% and 2.17%, respectively), which were regarded as background cell death due to regular stress during cell culture. (Fig. 5). This is mainly because we have taken unstained cells for gating and put the stained control cells in the FACS analysis as per the standard protocol [40,41]; (Ji et al., 2017).

Furthermore, morphological analysis with DAPI, Acridine orange, and Ethidium bromide staining demonstrated activation of apoptosis in MCF-7 cancer cells, characterised by condensed chromatin and many fragmented nuclei with BTN and DOX treatment in single and combination regimens (Fig. 6 and Fig. 7).

3.1.5. Both BTN and DOX bind tubulin

The innate ability of proteins to display the intrinsic fluorescence provided a way to understand the environmental changes after

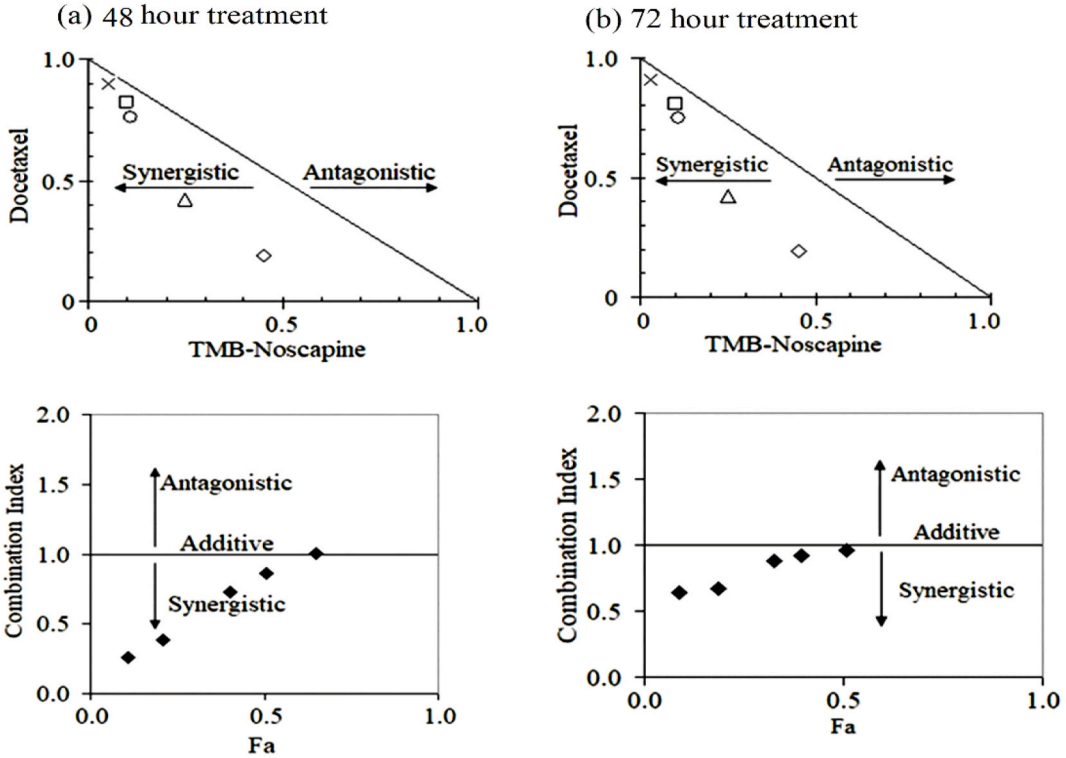

Fig. 3. Normalized isobologram for Br-TMB-Noscapine and DOX in the MCF-7 cell line. (A) The data points on the lower left on the diagonal line show synergistic effect. (B) In the plot between Fractional affected (Fa) and combination index (CI) using MCF-7 cell line, the data point below the horizontal line indicates synergistic effect.

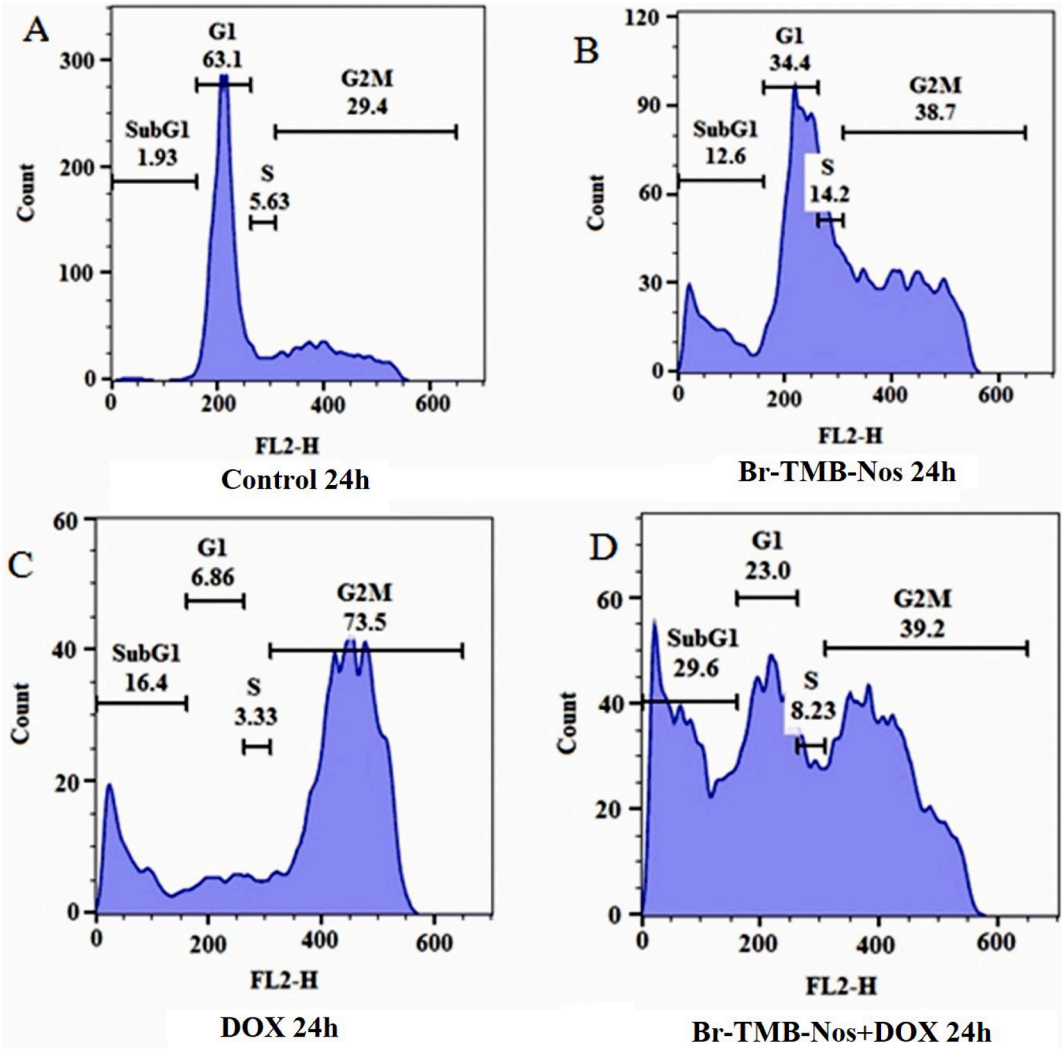

Fig. 4. Representative figure of flow-cytometry analysis for cell cycle progression with the treatment of BTN (10 μM) and DOX (0.1 μM) in single as well as combination (25 μM of BTN + 0.01 μM of DOX) for 24 h s. The cells were arrested in the G_2/M phase of cell cycle followed by the appearance of hypodiploid DNA peak (sub-G1) which indicate the apoptosis.

interaction with the quencher. Tubulin is autofluorescence due to the presence of tryptophan amino acid. Tryptophan (Trp), tyrosine (Tyr) and phenylalanine (Phe) are the three natural aromatic amino acids that are fluorescent in nature, but Trp does have the highest fluorescence quantum yield [42]. Any alteration in the conformation of protein due to ligand binding decreases the emission fluorescence - a standard tool used to recognize a ligand binding with protein. The decreased fluorescence intensity in the presence of increasing concentrations of BTN (10 μm, 25 μm) and DOX (0.1 μm) both in single and in combination tends to suggest the binding of both the compounds with tubulin. The percentage reduction in fluorescence intensity was 35.03%, 23.31% and 55% respectively in the presence of 10 μm BTN, 25 μm BTN and 0.1 μm DOX. Further reduction in fluorescence intensity of 69.9% and 79.2% respectively (Fig. 8) were observed in the combination treatment (DOX 0.01 μm + BTN 25 μm) and (DOX 0.001 μm + BTN 50 μm). The substantial decrease in tubulin fluorescence intensity in the combination treatment demonstrated the co-binding of both BTN and DOX with tubulin.

3.1.6. Effects of BTN and DOX in single and combination treatment altered the surface features of tubulin

In order to further examine the conformational changes in tubulin due to binding of BTN (10 μm and 25 μm) and DOX (0.1 μm) in single as well as in combination regimen, we probed the purified tubulin with ANS (8-anillino-1-naphthalenesulfonic acid). Treatment of tubulin with BTN and DOX in single and in combination demonstrated a significant improvement in tubulin-ANS fluorescence intensity (Fig. 9). It is reported an improvement in the fluorescence intensity was increased to 25% and 35.8% at 25 μM and 50 μM of BTN, 40.39% with 0.1 μM of DOX compared to unbound tubulin. In contrast, combination effect of both the compounds, DOX 0.01 μM + BTN 25 μM, DOX 0.001 μM + BTN 50 μM, increased the fluorescence intensity of the tubulin-ANS to 57% and 69%, respectively, demonstrating a progressive incremental disruption of the tubulin's structural integrity through linking the two agents together.

We investigated the impact of both drugs, BTN and DOX, on tubulin's secondary conformation using far-UV circular dichroism spectroscopy. Both compounds perturbed tubulin's secondary structure, as seen by restricted rotation of amino acids in tubulin treated with BTN (25 μM) and DOX (0.1 μM) alone and in their combination (25 μM BTN + 0.01 μM DOX). The elliptical shifts produced by BTN and DOX treatment, both alone or in combination, revealed a significant disruption in the structure of the alpha helix (Fig. 10), demonstrating that both compounds interact with the secondary structure of tubulin.

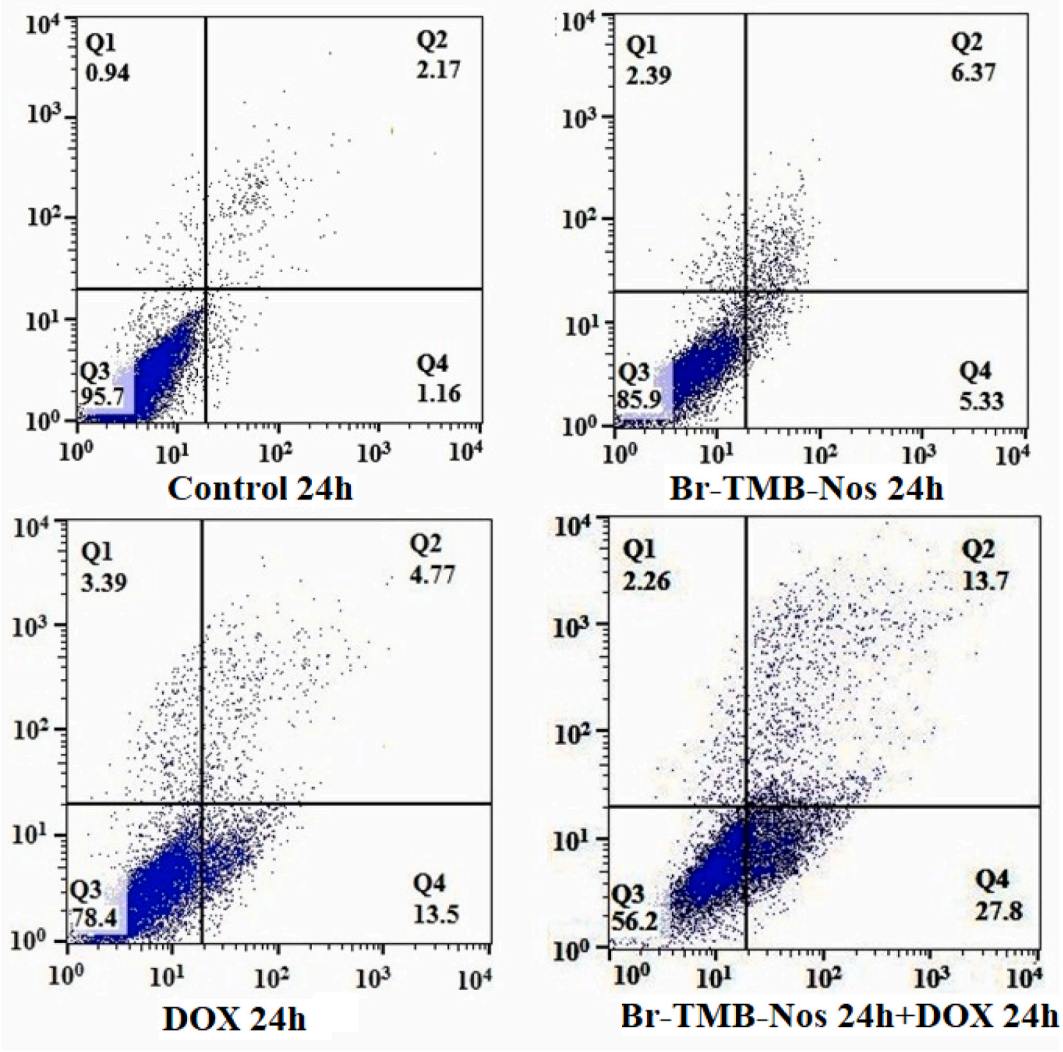

Fig. 5. Analysis of apoptosis cell death induced by Br-TMB-Nos (10 μM) and DOX (0.1 μM) and in combination (25 μM of Br-TMB-Nos + 0.01 μM of DOX) based on flow cytometric analysis. PE conjugate of Annexin V was used in combination with 7-Amino-Actinomycin (7-AAD) to distinguish among 3 subpopulations: PE^{-} and 7-AAD $^{-}$- population indicates viable cells (bottom left quadrant); PE $^{-}$- and 7-AAD + population indicates early apoptotic cells (lower right quadrant); PE + and 7-AAD + population indicate late apoptotic cells (top right quadrant).

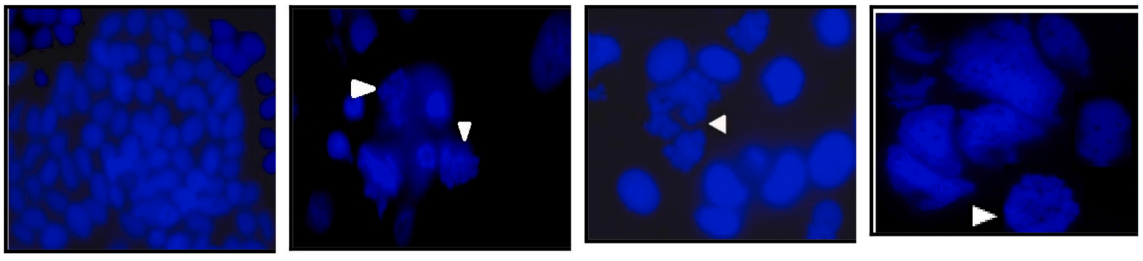

Fig. 6. The changes in morphological characters such as chromatin condensation, plasma membrane blebbing and appearance of small, apoptotic bodies indicated the apoptotic cells. Panels show morphological evaluation of nuclei stained with DAPI in the absence and presence of the Br-TMB-Nos (10 μM) and DOX (0.1 μM) in single as well as in combination regimen (25 μM Br-TMB-Nos + 0.01 μM DOX). Several typical features of apoptotic cells such as condensed chromosomes, numerous fragmented micronuclei, and apoptotic bodies are evident (indicated by white head arrows) upon 48 h of drug treatment. (Scale bar = 15 μm).

3.1.7. Reduction in tumor volume with treatment of BTN and DOX in single and in combination regimen against MCF-7 xenograft model

Treatment with BTN (150 mg/kg/day), DOX (1.5 mg/kg/week, i.v), or in combination (BTN 300 mg/kg/day + DOX 1.0 mg/kg/week, i.v) considerably decreased tumour volume in comparison to control ($P < 0.001$) (Fig. 12A). Tumor volume was reduced to 630 mm^3 with combination treatment, 960 mm^3 with DOX and 1145 mm^3 from the tumor size of 1630 mm^3 from the untreated control group on day 40 post

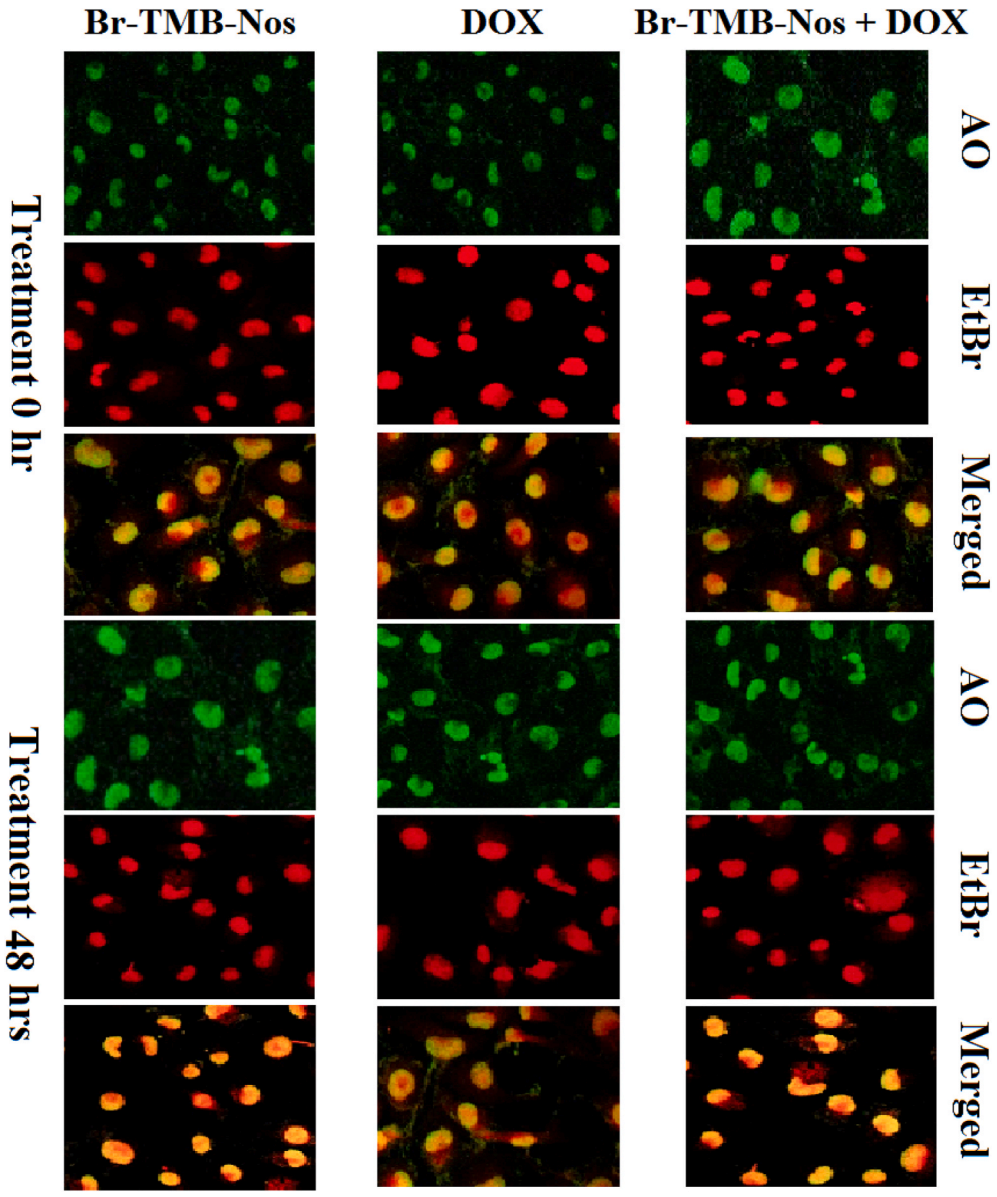

Fig. 7. The changes in morphological characters such as chromatin condensation, plasma membrane blebbing and appearance of small, apoptotic bodies indicated the apoptotic cells. Panels show morphological features of cells stained with AO, Etbr and merged channel of AO and EtBr. The apoptotic cancer cells were evident after 48 h of drug treatment.

tumour implantation. On 40th day tumor cell inoculation, mice were sacrificed and tumors were removed and weighted. All untreated mice developed solid tumors in sizes ranging from 4.5 g to 10.5 g (mean 7.8 ± 2.0 g). Whereas, among the treated groups the tumor size was significantly regressed and showed only small palpable tumors. Fig. 12B shows the mean tumor weight±standard error of control and experimental mice. Compared to untreated control mice, inhibition of tumor growth by the treatment of BTN and DOX in single or in combination regimen was statistically significant ($p < 0.001$). It is clear from these data that combination treatment of both BTN and DOX reduces the tumor size quite dramatically compared to single regimen treatment of BTN and DOX. In addition, we did not observe any apparent weight loss after drug treatment compared to the control group of mice (Fig. 12C).

3.1.8. Treatment of BTN and DOX in single and in combination does not cause any detectable toxicity

The severe side effects during chemotherapeutics are a major concern in the treatment of cancer patients. Tubulin binding agents for example, vinca alkaloids and taxanes, while clinically approved, are known to cause adverse side effects [43]. As a result, there is a need to identify a drug regimen that is both safe and well-tolerated. We examined the liver, kidney, spleen, lung, heart, brain, and colon of tumor-bearing mice to see if BTN and DOX in single or in combination treatment causes toxicity to normal tissues. Treatment with the compound BTN at daily doses of 150 mg/kg, DOX at a tolerated dose of 1.5 mg/kg body weight once in a week and in their combination treatment (BTN 300 mg/kg/day + DOX 1.0 mg/kg/week, i.v.) fails to reveal any detectable pathological abnormalities in normal tissues involved in normal cell proliferation. H&E staining of paraffin-embedded 5.0 micron-thick sections of the liver, kidney, spleen, lung, heart, colon, and brain is shown at 200x magnification in Fig. 11. Brain microsections revealed no infracted regions. The hepatic lobular architecture was normal. Normal glomeruli, proximal and distal tubules, interstitium, and blood vessels were found in the kidneys. Among the groups, the heart muscle exhibited normal morphology. Normal alveoli and bronchial airways have been seen in the lung tissue. Furthermore, we

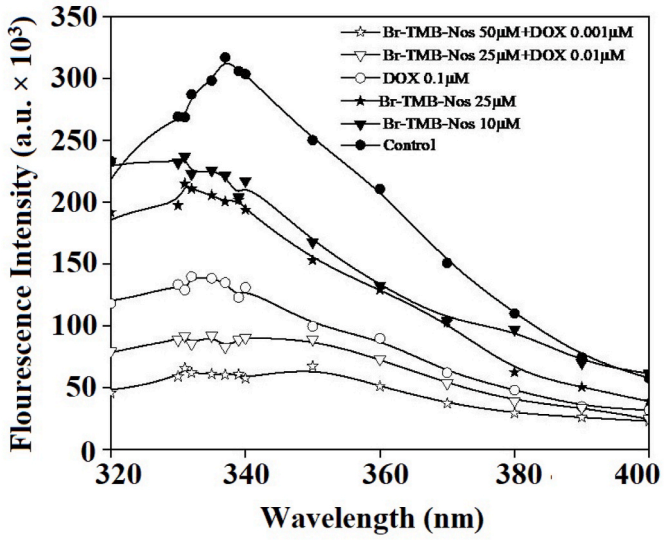

Fig. 8. Decrease of fluorescence intensity of tubulin by Br-TMB-Nos and DOX in single as well as in combination regimen. Tubulin (2.0 μM) was incubated with Br-TMB-Nos (10 μM and 25 μM) and DOX (0.1 μM) alone as well as in combination regimen (25 μM of Br-TMB-Nos + 0.01 μM of DOX and 50 μM of Br-TMB-Nos + 0.001 μM of DOX) and the emission spectra were collected (310 nm–400 nm). Both Br-TMB-Nos and DOX in single as well as in combination regimen showed a concentration-dependent quenching of the intrinsic tubulin fluorescence emission intensity indicating the binding of both Br-TMB-Nos and DOX to tubulin. The more reduction in tubulin fluorescence intensity in combination regimen of both Br-TMB-Nos and DOX, compared to their single binding, revealed combination effect with the tubulin. The graph is a representative of three independent experiments.

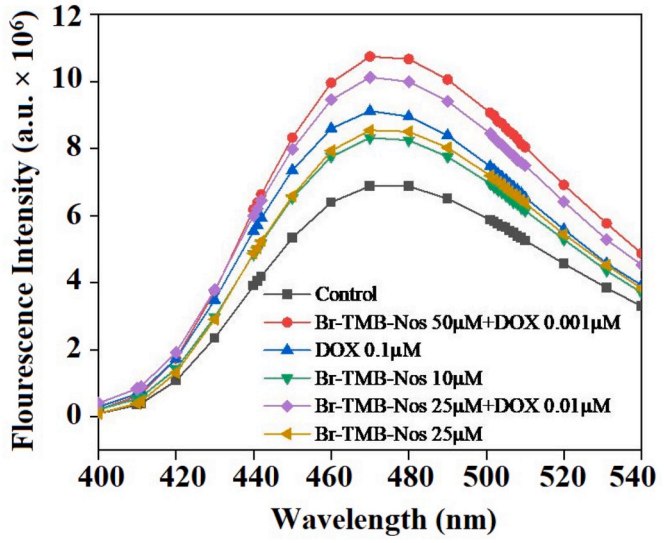

Fig. 9. Enhancement of tubulin-ANS fluorescence by Br-TMB-Nos and DOX in single as well as in combination regimen. Tubulin (2.0 μM) was incubated without (control) or with Br-TMB-Nos (10 μM and 25 μM), DOX (0.1 μM) and in their combination regimen (Br-TMB-Nos 25 μM + DOX 0.01 μM, Br-TMB-Nos 50 μM + DOX 0.001 μM), followed by incubation with ANS (50 μM). The samples were excited at 380 nm and the emission spectra were collected (390 nm–500 nm). Both Br-TMB-Nos and DOX in single as well as in combination regimen showed a concentration-dependent increase in tubulin-ANS fluorescence indicating the binding of both Br-TMB-Nos and DOX to tubulin. The increase is more in tubulin-ANS fluorescence in combination regimen of both Br-TMB-Nos and DOX, compared to their single binding, revealed combination effect with the tubulin. The graph is a representative of three independent experiments.

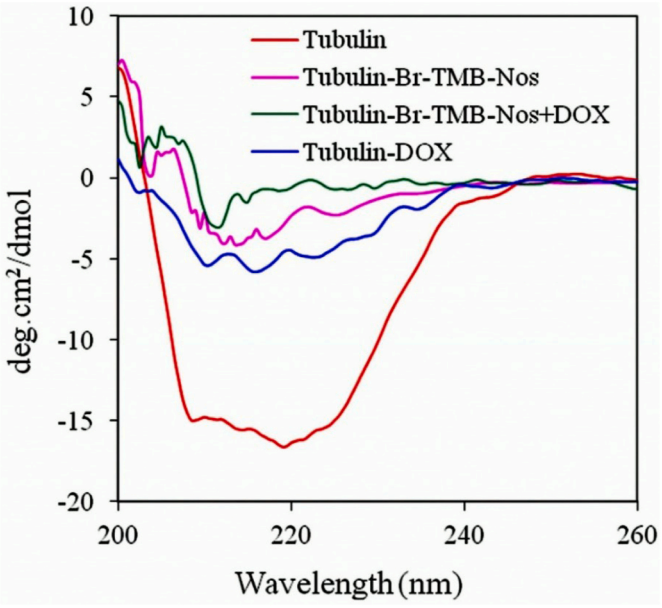

Fig. 10. Characterization of Br-TMB-Nos (25 μM) and DOX (0.1 μM) in single as well as in combination regimen (25 μM of Br-TMB-Nos + 0.01 μM of DOX) –tubulin interactions in single as well as in combination. Far-UV circular dichroism spectra indicating disruption of tubulin secondary structure by Br-TMB-Nos and DOX. The graph represents one of the three independent experiments.

observed differences in hematological parameters between treated and control animals.

3.2. (B)

3.2.1. Molecular modelling

Noscapinoids bind at the α- and β-tubulin interfaces, while docetaxel binding is biased to β-tubulin [28]. In order to determine the binding score of both ligands individually and in combination, we docked them in three cycles of molecular docking at their appropriate binding pocket on tubulin. DOX and BTN were docked into their respective binding pockets separately in the first cycle. Both BTN and DOX docked well into their respective binding sites, with docking scores of −4.37 kcal/mol and −5.74 kcal/mol (Table 1). The difference in docking scores in presence of DOX in second cycle, indicate the binding score is improves due to the binding of DOX, altered to −7.24 kcal/mol. Similarly, in the third cycle, DOX was docked into its binding pocket in the tubulin-BTN co-complex to evaluate to see how its docking score altered in the presence of BTN. The presence of BTN further lowered the docking score of DOX to −6.44 kcal/mol (Table 1).

3.2.2. Molecular dynamics simulation

A molecular dynamic simulation of 100 ns was used to analyse the binding of the both BTN and DOX to tubulin (Tub-BTN and Tub-DOX complexes) or in combination with tubulin (Tub-DOX + BTN). To evaluate the stability of the system, the root means square deviations (RMSD) and the root means square fluctuations (RMSF) of Cα-atoms were computed for all frames throughout the simulation (Fig. 13 and Fig. 14). Both BTN and DOX were shown to bind to tubulin throughout the simulation. Both BTN and DOX were reported to fit well within the binding cavity. The BTN docked effectively at the interface of α- and β-tubulin, while DOX binding is more oriented towards β-tubulin (Fig. 15 a, b). Their binding strategy with tubulin was illustrated by ligplots in both individual and combination forms (Fig. 16). Ligplot showed the hydrogen and hydrophobic bonds of the individual ligands and the amino acids involved in their binding sites. Two hydrogen bonds

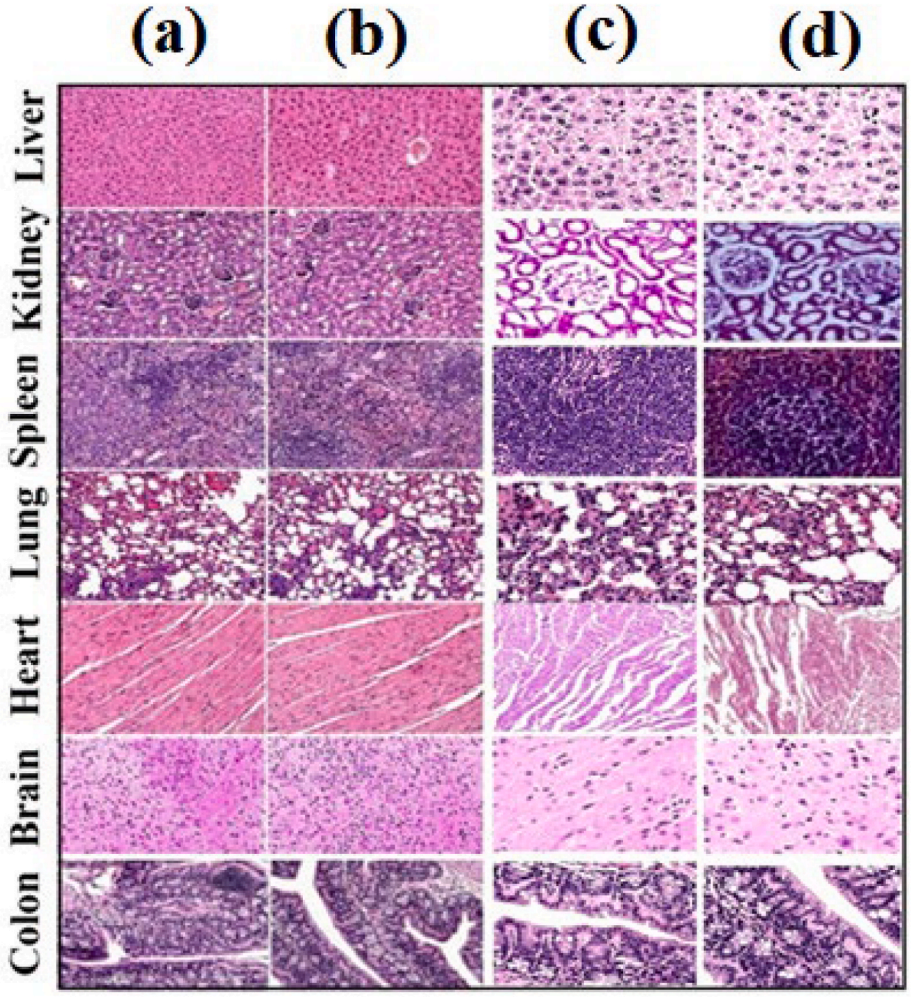

Fig. 11. Represent H&E staining of paraffin-embedded 5.0 micron-thick sections of (a)Vehicle, (b) Br-TMB-Nos (150 mg/kg/day), (c) DOX (1.5 mg/kg/week), (d) (Br-TMB-Nos 300 mg/kg/day + DOX 1.0 mg/kg/week), the colon, brain, heart, lung, spleen, kidney and liver at a magnification of 200x.

contributed to the interactions of BTN with the binding pocket of tubulin. The amino acids present in the binding site involved in the binding of BTN are Glu 345(D), Asn 337(D), Leu 333(D), Pro 175(D), Glu 176(A), Ser 340(D), Val 351(D), Glu 336(D), Phe 343(D). Two binding site amino acids, Asn 349(D) and Asn 350(D) provided two hydrogen bonds to strengthen the binding of BTN to tubulin with a distance of 2.65 Å and 2.95 Å, respectively. Likewise, the binding of DOX involves two hydrogen bonds with a distance of 2.86 Å with the amino acids Arg 369 D and Gly 370 D. The respective amino acids involved in the binding of DOX are His 229(D), Lys 372 (D), Leu 286 (D), Arg 284(D), Pro 274(D), Leu 371 (D), Gln 281 (D), Thr 276 (D), Leu 217 (D), Pro 360 (D). In comparison, there is a significant difference in the amino acids involved in the interaction of BTN as well as DOX in the co-complex of tubulin with both the ligands.

3.2.3. Post scoring with MM-GBSA and MM-PBSA

The binding free energy and its constituents for both BTN and DOX with tubulin were computed individually and in combination and are shown in Table 2. Using both the MM-GBSA and MM-PBSA approaches, the overall average of the free energy of binding was calculated utilizing a last 250 frames from the last 5 ns of trajectories. The binding free energy for BTN and DOX with tubulin was found to be −25.69 and −38.17 kcal/mol based on MM-GBSA as well as −29.11 and −36.60 kcal/mol based on MM-PBSA, respectively. Further, the binding free energy of BTN was reduced to −30.02 and −33.54 kcal/mol using MM-GBSA and MM-PBSA calculation when DOX was present on its binding pocket, indicating combination effect of both the ligands. Parenthetically, the free energy of binding of DOX was reduced to −39.17 and −35.80 kcal/mol using MM-GBSA and MM-PBSA, respectively when BTN was present in binding with tubulin. The calculated binding free energy was splitted into its numerous energy components such as the electrostatic, van der Waals, and solvation. Both van der Waals (ΔE_{VDW}) and the electrostatic component (ΔE_{ELE}) were known to contributed significantly to the binding free energy. However, the net polar contribution ($\Delta G_{(ele,PB/GB)} = \Delta E_{ele} + \Delta G_{(PB/GB)}$) was rendered unfavourable due to very large penalty imposed by the desolvation component ($\Delta G_{PB/GB}$) while the net nonpolar component (ΔE_{vdw}) and ($\Delta G_{sol\text{-}np}$) were observed to make a highly favourable contribution to the free energy of binding.

It is a surprise and interesting finding that the two ligands, BTN and DOX bind at two different binding sites on tubulin, yet they can synergize the effect. The confusion is mainly because BTN binds tubulin at the colchicine-binding site and colchicine is a microtubule depolymerizing drug. This effect of colchicine is quite opposite to that of DOX which is a polymerization promoting drug. However, it is clearly well documented by independent workers the two microtubule drugs, paclitaxel and noscapine, showed synergistic effect on prostate cancer (LNCaP and PC-3) and also on ovarian cancers [2,44]. Likewise, there are clear credible reports of synergism between noscapine and another microtubule interacting drugs vinca-alkaloids on other types of cancers [45].

It was previously reported that the microtubule interacting drugs i.e., paclitaxel and its derivative DOX as well as noscapine and its derivatives

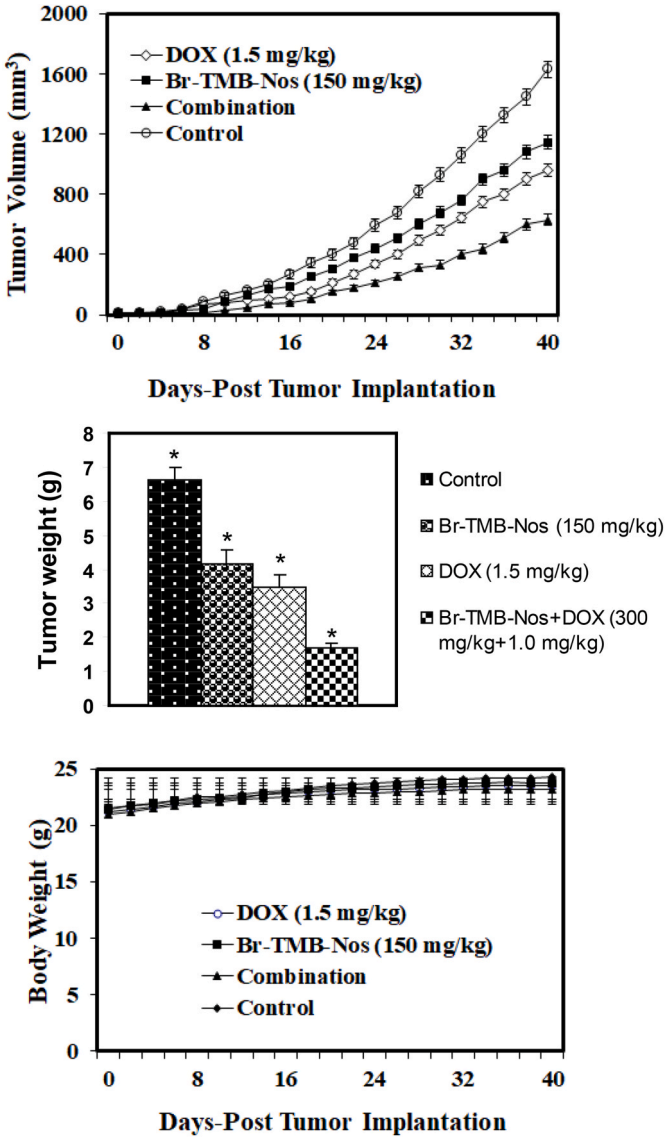

Fig. 12. (A) Progression profile of tumor growth kinetics of in-vivo antitumor effect of therapeutics doses of Br-TMB-Nos and DOX alone and in combination regimen on human MCF-7 tumor xenograft model (tumor volumes, mm^3 ± SEM), (B) and measurement of body weight following Br-TMB-Nos alone, DOX alone and in combination regimen.Female nude mice with xenograft MCF-7 tumors received various treatments for 30 days starting on day 7 post tumor implantation. The mice were treated with Br-TMB-Nos (150 mg/kg/day), DOX (1.5 mg/kg i.v.) and Br-TMB-Nos 300 mg/kg/day + DOX 1.0 mg/kg/week. Control group received vehicle only. Statistical significance of the difference in tumor volume of treatment groups compared with control. $P < 0.01$ (*, significantly different from untreated controls; **, significantly different from Br-TMB-Nos and DOX single treatments). This experiment was repeated twice.

bind at distinct places on the dimmers of tubulin [46]. It was also demonstrated that noscapine and its derivatives bind at a site overlapping with colchicine binding site at the interface between α- and β-tubulin [20,21,26]. However, the effect of colchicine-binding on microtubule dynamics is quite distinct from the effect of noscapine or its derivative, BTN. While most of the tubulin subunits bound to colchicine depolymerize (except for one terminal colchicine-tubulin at each protofilament) noscapine can bind stoichiometrically to tubulin which is capable of polymerization into normal looking (although somewhat flexible microtubule lattice) [1]. Further, colchicine at very low sub-stoichiometric concentrations was found to leave microtubule-polymer mass intact and only modulate dynamics.

Table 1
Molecular docking results (Glide XP_{score}) and the relevant energy parameters of BTN and DOX in single as well as in combination with tubulin.

Ligands	Glide XP_{score} (kcal/mol)	Glide E_{vdw} (kcal/mol)	Glide E_{coul} (kcal/mol)	Glide Energy (kcal/mol)
BTN	−4.37	−42.758	−6.445	−49.202
DOX	−5.74	−37.737	−5.176	−42.914
BTN docked with Tubulin_DOX complex	−7.24	−45.902	−11.713	−57.615
DOX docked with BTN complex	−6.44	−25.078	−9.396	−25.474

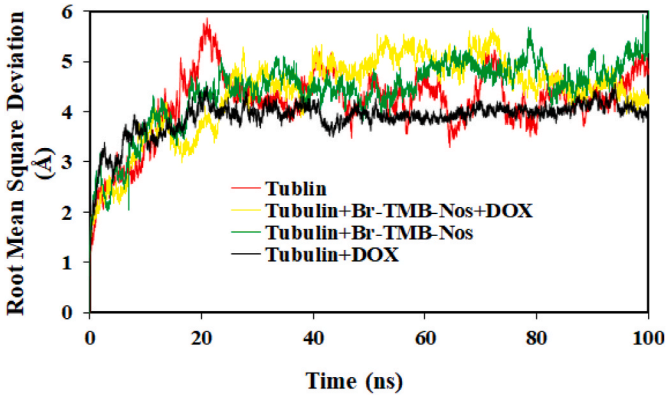

Fig. 13. Root mean square deviations (RMSD) of Cα carbon atoms of tubulin only and in complex with Br-TMB-Nos (Tubulin + Br-TMB-Nos), with docetaxel (Tubulin + DOX) and with both docetaxel and Br-TMB-Nos (Tubulin + DOX + Br-TMB-Nos) during 100 ns of MD simulation. The relative fluctuation in the RMSD of the Cα atoms is very small after ~20 ns of the simulation. The time step of 20 ps was used during the simulation. The topmost 5 frames from the MD simulation trajectory with lowest total energy were considered to generate the average structure.

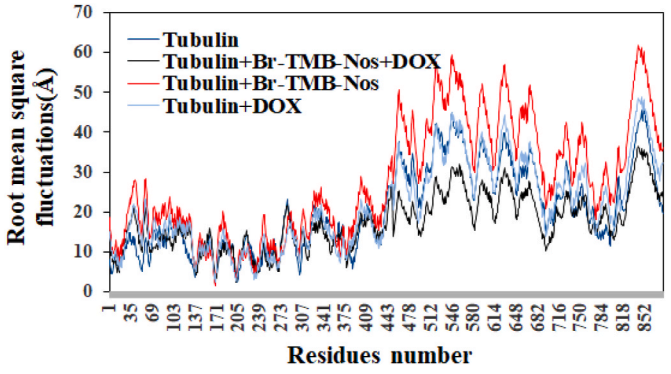

Fig. 14. Root mean square fluctuation (RMSF) of the residues of tubulin of the docked ligands in the bound form and in the unbound form of tubulin heterodimer. Different levels of flexibility of these residues were noticed in the bound form of tubulin with Br-TMB-Nos and DOX in single as well as in combination. Most of the residues showed flexibilities >5 Å in case of tubulin bound with Br-TMB-Nos and DOX as compared to the free tubulin heterodimer, indicating that these residues seem to be more flexible as a result of binding.

Noscapine on the other hand can modulate microtubule-assembly even at high stoichiometric concentrations [6]. In contrast, ppaclitaxel binds on microtubule surface lattice on the luminal side of the microtubule near the lateral interaction site of the protofilaments thus stabilizing MT lattice against depolymerization.

Although a lot of definitive experimental and modeling work

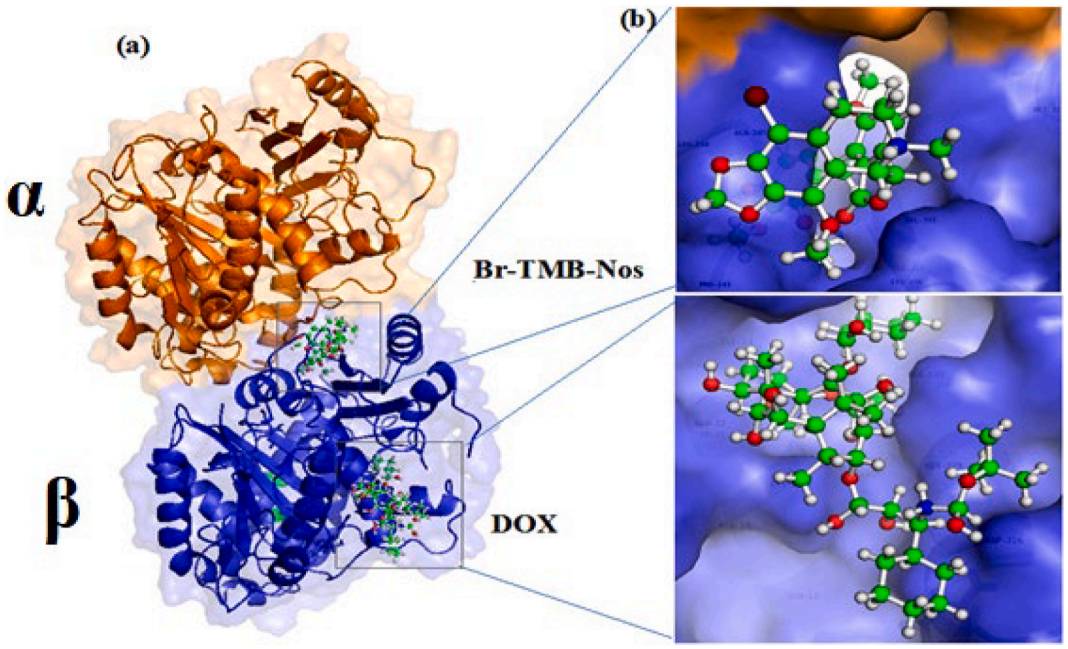

Fig. 15. (a) Br-TMB-Nos and DOX are well accommodated inside their respective binding site of tubulin. (b) Snapshot of both the ligands obtained. The binding site is represented as macromodel surface according to α- and β-tubulin (α-tubulin is represented in brown colour and β-tubulin is represented in blue colour).

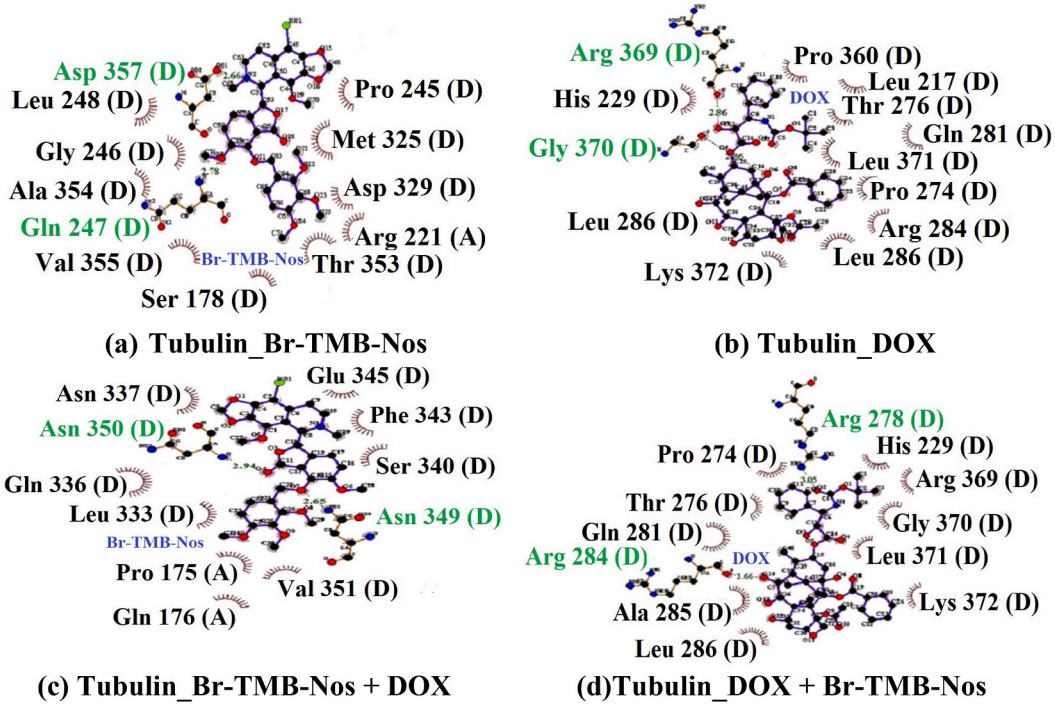

Fig. 16. The ligplot analysis showing the binding mode of (a) Br-TMB-Nos in single and (b) DOX in single. The binding site residues involved in the interaction of Br-TMB-Nos are slightly different in combination with DOX. Similarly, the ligplot analysis showing the binding mode of (c) Br-TMB-Nos when it is docked into the co-complex of tubulin and DOX (d) DOX when it is docked into the co-complex of tubulin and Br-TMB-Nos. The binding site residues involved in the interaction of DOX are slightly different in combination with Br-TMB-Nos. The hydrogen bonds formed (if any) are represented as dotted lines.

remains to be done but it is quite reasonable hypothesis that paclitaxel (and DOX) and noscapine (or BTN) can bind simultaneously. Of course, it is also possible, that mechanisms independent of tubulin/microtubule contribute to the synergism. Multiple cellular processes/mechanisms such as hypoxia, stress response including C-Jun N-terminal kinase, apoptosis, autophagy, etc. have shown subtle changes as an effect of parent molecules noscapine as well as taxol.

4. Conclusion

The extensive molecular modelling, cellular, biochemical studies and *in vivo* animal experimental studies revealed the combination effect of one of the derivatives of noscapine (BTN) and docetaxel compensating for the lack of previous DOX-based combination therapy studies. Meanwhile, the synergistic effect of BTN + DOX have been extensively

Table 2
Predicted free energy of binding ($\Delta G_{bind,pred}$) and its various components (kcal/mol) of BTN and DOX in single as well as in combination binding with tubulin. The values in bold represent the ($\Delta G_{bind,pred}$) of molecules with tubulin based on MM-GBSA and MM-PBSA methods.

Energy Component	BTN	DOX	Tub_DOX + BTN	Tub_ BTN + DOX
ΔE_{VDW}	−32.61	−40.26	−40.44	−37.07
ΔE_{ELE}	−280.66	−14.23	−333.55	−35.00
ΔE_{GAS}	−313.34	−52.26	−344.44	−60.45
$\Delta G_{GB\text{-}Polar}$	318.85	25.50	317.49	30.98
$\Delta G_{SOL\text{-}NP}$	−3.72	−4.65	−3.70	−4.55
$\Delta G_{SOL\text{-}GB}$	270.32	27.29	303.70	31.53
$\Delta G_{bind\text{-}GBSA}$	**−25.69**	**−38.17**	**−30.02**	**−39.17**
ΔG_{PB}	313.06	30.02	323.44	30.09
$\Delta G_{SOL\text{-}NP}$	−3.44	−4.71	−3.46	−4.09
$\Delta G_{SOL\text{-}PB}$	270.12	25.51	328.28	32.09
$\Delta G_{bind\text{-}PBSA}$	**−29.11**	**−36.60**	**−33.54**	**−35.80**

elucidated for the first time. Stable interaction was revealed in molecular dynamic simulation for 100 ns from both of the ligands with tubulin. These findings corroborate the inhibition of noscapine analogues on tubulin organization into microtubules, as well as the subsequent cellular implications, which are done through the same biochemical pathways. All these findings in our study might form a theoretical basis for the combination of BTN and DOX. Inhibiting proliferative activity was substantially enhanced when both the drugs used in combination as compared to their single regimen treatment. Both the ligands also have been found to bind with tubulin efficiently at combination treatment. We used a normal therapeutic dose of BTN 150 mg/kg/day administered by oral gavage and DOX 1.5 mg/kg/week administered by i.v. injection to assess the combination potential of the two drugs in context to their anticancer efficacy in MCF-7 xenograft tumors in nude mice. Our *in vivo* results demonstrated that a combination has a synergistic effect on a murine breast cancer model induced by the MCF-7. Surprisingly, non-significant change in weight loss for BTN, DOX, and in their combination treatment, indicating that BTN and DOX have a favourable toxicity profile. Brought together, concrete evidence has been established that a reasonable combination of BTN and DOX could produce synergistic effects on cancer therapies, which is extremely encouraging for improving therapeutic potential in preclinical and clinical research.

Declaration

The work was supported by the Department of Science and Technology, Govt. of India, grant no: DST/INSPIRE/Code No.: IF170022.

Declaration of competing interest

The authors declare that they have no conflicts of interest that are relevant to the content of this article. All data generated or analysed during this study are included in this article.

Acknowledgments

We would like to acknowledge the financial support provided by the OHEPEE, Govt. of Odisha through the World Bank. Shruti Gamya Dash wishes to acknowledge the award of fellowship by the Department of Science and Technology, Govt. of India, (DST/INSPIRE/Code No.: IF170022). We are grateful to Dr Manu Lopus, UM-DAE Centre for Excellence in Basic Sciences for providing extended facilities.

References

[1] K. Ye, Y. Ke, N. Keshava, J. Shanks, J.A. Kapp, R.R. Tekmal, J. Petros, H.C. Joshi, Opium alkaloid noscapine is an antitumor agent that arrests metaphase and induces apoptosis in dividing cells, Proc. Natl. Acad. Sci. U.S.A. 95 (1998) 1601–1606.

[2] J. Zhou, K. Gupta, J. Yao, K. Ye, D. Panda, P. Giannakakou, H.C. Joshi, Paclitaxel-resistant human ovarian cancer cells undergo c-Jun NH2-terminal kinase-mediated apoptosis in response to noscapine, J. Biol. Chem. 277 (42) (2002) 39777–39785, https://doi.org/10.1074/jbc.M203927200.

[3] J.W. Landen, V. Hau, M. Wang, T. Davis, B. Ciliax, B.H. Wainer, E.G. Van Meir, J. D. Glass, H.C. Joshi, D.R. Archer, Noscapine crosses the blood-brain barrier and inhibits glioblastoma growth, Clin. Cancer Res. : Off. J. Am. Assoc. Canc. Res. 10 (15) (2004) 5187–5201, https://doi.org/10.1158/1078-0432.CCR-04-0360.

[4] M.A. Jordan, L. Wilson, Microtubules as a target for anticancer drugs, Nat. Rev. Cancer 4 (4) (2004) 253–265, https://doi.org/10.1038/nrc1317. PMID: 15057285.

[5] Y. Ke, K. Ye, H.E. Grossniklaus, D.R. Archer, H.C. Joshi, J.A. Kapp, Noscapine inhibits tumor growth with little toxicity to normal tissues or inhibition of immune responses, Cancer Immunol. Immunother. : CII 49 (4–5) (2000) 217–225, https://doi.org/10.1007/s002620000109.

[6] J. Zhou, K. Gupta, S. Aggarwal, R. Aneja, R. Chandra, D. Panda, H.C. Joshi, Brominated derivatives of noscapine are potent microtubule-interfering agents that perturb mitosis and inhibit cell proliferation, Mol. Pharmacol. 63 (4) (2003) 799–807, https://doi.org/10.1124/mol.63.4.799.

[7] Martindale: The extra pharmacopoeia. 27th ed. Edited by Ainley Wade and James E. F. Reynolds. The Pharmaceutical Press, 1 Lambeth High Street, London, SEI 7JN, England, 1977.19 × 25.4 cm. 2077 pp. Price $60. Available from Rittenhouse Book Distributors, 251 S. 24th St., Philadelphia, PA 19103.

[8] B. Dahlström, T. Mellstrand, C.G. Löfdahl, M. Johansson, Pharmacokinetic properties of noscapine, Eur. J. Clin. Pharmacol. 22 (6) (1982) 535–539, https://doi.org/10.1007/BF00609627. PMID: 7128665.

[9] P.C. Rida, D. LiVecche, A. Ogden, J. Zhou, R. Aneja, The noscapine chronicle: a pharmaco-historic biography of the opiate alkaloid family and its clinical applications, Med. Res. Rev. 35 (5) (2015) 1072–1096, https://doi.org/10.1002/med.21357.

[10] T. Hida, K. Kozaki, H. Ito, O. Miyaishi, Y. Tatematsu, T. Suzuki, K. Matsuo, T. Sugiura, M. Ogawa, T. Takahashi, T. Takahashi, Significant growth inhibition of human lung cancer cells both in vitro and in vivo by the combined use of a selective cyclooxygenase 2 inhibitor, JTE-522, and conventional anticancer agents, Clin. Cancer Res. 8 (7) (2002) 2443–2447.

[11] S.T. Nawrocki, B. Sweeney-Gotsch, R. Takamori, D.J. McConkey, The proteasome inhibitor bortezomib enhances the activity of docetaxel in orthotopic human pancreatic tumor xenografts, Mol. Cancer Therapeut. 3 (2004) 59–70.

[12] C.J. Sweeney, S. Mehrotra, M.R. Sadaria, S. Kumar, N.H. Shortle, Y. Roman, C. Sheridan, R.A. Campbell, D.J. Murry, S. Badve, H. Nakshatri, The sesquiterpene lactone parthenolide in combination with docetaxel reduces metastasis and improves survival in a xenograft model of breast cancer, Mol. Cancer Therapeut. 4 (6) (2005) 1004–1012.

[13] M.S. Shaik, A. Chatterjee, T. Jackson, M. Singh, Enhancement of antitumor activity of docetaxel by celecoxib in lung tumors, Int. J. Cancer 118 (2006) 396–404.

[14] M. Chougule, A.R. Patel, P. Sachdeva, T. Jackson, M. Singh, Anticancer activity of Noscapine, an opioid alkaloid in combination with Cisplatin in human non-small cell lung cancer, Lung Cancer 71 (3) (2011) 271–282.

[15] T. Mahaddalkar, P.K. Naik, S. Choudhary, N. Manchukonda, S. Kantevari, M. Lopus, Structural investigations into the binding mode of a novel noscapine analogue, 9-(4-vinylphenyl) noscapine, with tubulin by biochemical analyses and molecular dynamic simulations, J. Biomol. Struct. Dyn. 35 (11) (2017) 2475–2484, https://doi.org/10.1080/07391102.2016.1222969. Epub 2016 Aug 31. PMID: 27576773.

[16] S.G. Dash, C. Suri, P.K.R. Nagireddy, S. Kantevari, P.K. Naik, Rational design of 9-vinyl-phenyl noscapine as potent tubulin binding anticancer agent and evaluation of the effects of its combination on Docetaxel, J. Biomol. Struct. Dyn. 39 (14) (2020) 5276–5289, https://doi.org/10.1080/07391102.2020.1785945.

[17] S.G. Dash, S. Kantevari, S.K. Pandey, P.K. Naik, Synergistic interaction of N-3-Br-benzyl-noscapine and docetaxel abrogates oncogenic potential of breast cancer cells, Chem. Biol. Drug Des. 98 (3) (2021) 466–479, https://doi.org/10.1111/cbdd.13902.

[18] R. Aneja, M. Lopus, J. Zhou, S.N. Vangapandu, A. Ghaleb, J. Yao, J.H. Nettles, B. Zhou, M. Gupta, D. Panda, R. Chandra, H.C. Joshi, Rational design of the microtubule-targeting anti–breast cancer drug EM015, Cancer Res. 66 (7) (2006) 3782–3791.

[19] M.M. Tomayko, C.P. Reynolds, Determination of subcutaneous tumor size in athymic (nude) mice, Cancer Chemother. Pharmacol. 24 (3) (1989) 148–154, https://doi.org/10.1007/BF00300234. PMID: 2544306.

[20] P.K. Naik, B.P. Chatterji, S.N. Vangapandu, R. Aneja, R. Chandra, S. Kantevari, H. C. Joshi, Rational design, synthesis and biological evaluations of amino-noscapine: a high affinity tubulin-binding noscapinoid, J. Comput. Aided Mol. Des. 25 (5) (2011) 443–454.

[21] P.K. Naik, S. Santoshi, A. Rai, H.C. Joshi, Molecular modelling and competition binding study of Br-noscapine and colchicine provide insight into noscapinoid-tubulin binding site, J. Mol. Graph. Model. 29 (2011) 947–955. http://doi: 10.1016/j.jmgm.2011.03.004.

[22] C. Lee, W. Yang, R.G. Parr, Development of the Colle-Salvetti correlation-energy formula into a functional of the electron density, Phys. Rev. B Condens. Matter 3 (1988) 785–789.

[23] A.D. Becke, A new mixing of Hartree-Fock and local density-functional theories, J. Chem. Phys. 98 (1993) 1372–1377.

[24] J.S. Binkley, J.A. Pople, W.J. Hehre, Self-consistent molecular orbital methods. 21. Small split-valence basis sets for first-row elements, J. Am. Chem. Soc. 102 (1980) 939–947.

[25] W.J. Pietro, M.M. Francl, W.J. Hehre, D.J. Defrees, J.A. Pople, J.S. Binkley, Self-consistent molecular orbital methods. 24. Supplemented small split-valence basis sets for second-row elements, J. Am. Chem. Soc. 104 (1982) 5039–5048.
[26] M.A. Oliva, A.E. Prota, J. Rodriguez Salarichs, Y.L. Bennani, J. Jimenez barbero, K. Bargsten, A. Canales, M.O. Steinmetz, J.F. Diaz, Structural basis of noscapine activation for tubulin binding, J. Med. Chem. (63) (2020) 8495–8501.
[27] S. Santoshi, P.K. Naik, Molecular insight of isotypes specific β-tubulin interaction of tubulin heterodimer with noscapinoids, J. Comput. Aided Mol. Des. 28 (2014) 751–763.
[28] J.P. Snyder, J.H. Nettles, B. Cornett, K.H. Downing, E. Nogales, The binding conformation of Taxol in tubulin: a model based on electron crystallographic density, Proc. Natl. Acad. Sci. U.S.A. 98 (9) (2001) 5312–5316.
[29] R.A. Friesner, J.L. Banks, R.B. Murphy, T.A. Halgren, J.J. Klicic, D.T. Mainz, M. P. Repasky, E.H. Knoll, M. Shelley, J.K. Perry, D.E. Shaw, P. Francis, P.S. Shenkin, Glide: a new approach for rapid, accurate docking and scoring. 1. Method and assessment of docking accuracy, J. Med. Chem. 47 (7) (2004) 1739–1749, https://doi.org/10.1021/jm0306430.
[30] T.A. Halgren, R.B. Murphy, R.A. Friesner, H.S. Beard, L.L. Frye, W.T. Pollard, J. L. Banks, Glide: a new approach for rapid, accurate docking and scoring. 2. Enrichment factors in database screening, J. Med. Chem. 47 (2004) 1750–1759, https://doi.org/10.1021/jm030644s.
[31] D.A. Case, R.M. Betz, D.S. Cerutti, T.E. Cheatham III, T.A. Darden, R.E. Duke, T. J. Giese, H. Gohlke, A.W. Goetz, N. Homeyer, S. Izadi, P. Janowski, J. Kaus, A. Kovalenko, T.S. Lee, S. LeGrand, P. Li, C. Lin, T. Luchko, R. Luo, B. Madej, D. Mermelstein, K.M. Merz, G. Monard, H. Nguyen, H.T. Nguyen, I. Omelyan, A. Onufriev, D.R. Roe, A. Roitberg, C. Sagui, C.L. Simmerling, W.M. Botello-Smith, J. Swails, R.C. Walker, J. Wang, R.M. Wolf, X. Wu, L. Xiao, P.A. Kollman, AMBER. 2016, University of California, San Francisco, 2016.
[32] J. Wang, W. Wang, P.A. Kollman, D.A. Case, Automatic atom type and bond type perception in molecular mechanical calculations, J. Mol. Graph. Model. 25 (2006) 247–260.
[33] A. Jakalian, D.B. Jack, C.I. Bayly, Fast, efficient generation of high-quality atomic charges. AM1-BCC model: II. Parameterization and validation, J. Comput. Chem. 23 (2002) 1623–1641, https://doi.org/10.1002/jcc.10128.
[34] W.L. Jorgensen, J. Chandrasekhar, J.D. Madura, R.W. Impey, M.L. Klein, Comparison of simple potential functions for simulating liquid water, J. Chem. Phys. 79 (1983) 926–935, https://doi.org/10.1063/1.445869.
[35] J.A. Maier, C. Martinez, K. Kasavajhala, L. Wickstrom, K.E. Hauser, C. Simmerling, ff14SB: improving the accuracy of protein side chain and backbone parameters from ff99SB, J. Chem. Theor. Comput. 11 (2015) 3696–3713, https://doi.org/10.1021/acs.jctc.5b00255.
[36] J.P. Ryckaert, G. Ciccotti, H.J. Berendsen, Numerical integration of the cartesian equations of motion of a system with constraints: molecular dynamics ofn-alkanes, J. Comput. Phys. 23 (1977) 327–341, https://doi.org/10.1016/0021-9991(77)90098-5.
[37] T. Darden, D. York, L. Pedersen, Particle mesh Ewald: an N. log (N) method for Ewald sums in large systems, J. Chem. Phys. 98 (1993) 10089–10092, https://doi.org/10.1063/1.464397.
[38] U. Essmann, L. Perera, M.L. Berkowitz, T. Darden, H. Lee, L.G. Pedersen, A Smooth particle mesh: Ewald method, J. Chem. Phys. 103 (1995) 8577–8593, https://doi.org/10.1063/1.470117.
[39] P.A. Kollman, I. Massova, C. Reyes, B. Kuhn, S. Huo, L. Chong, M. Lee, T. Lee, Y. Duan, W. Wang, Calculating structures and free energies of complex molecules: combining molecular mechanics and continuum models, Accounts Chem. Res. 33 (12) (2000) 889–897, https://doi.org/10.1021/ar000033j.
[40] N. Sivakumaran, S.R. Samarakoon, A. Adhikari, M.K. Ediriweera, K.H. Tennekoon, N. Malavige, I. Thabrew, R.L.S. Shrestha, Cytotoxic and apoptotic effects of govaniadine isolated from Corydalis govaniana wall. Roots on human breast cancer (MCF-7) cells, BioMed Res. Int. (2018) 1–11.
[41] B. Fan, S. Shi, X. Shen, X. Yang, N. Liu, G. Wu, X. Guo, N. Huang, Effect of HMGN2 on proliferation and apoptosis of MCF-7 breast cancer cells, Oncol. Lett. 17 (1) (2019) 1160–1166.
[42] D. Sood, N. Kumar, G. Rathee, et al., Mechanistic interaction study of bromo-noscapine with bovine serum albumin employing spectroscopic and chemoinformatics approaches, Sci. Rep. 8 (2018), 16964, https://doi.org/10.1038/s41598-018-35384-6.
[43] E.K. Rowinsky, The development and clinical utility of the taxane class of antimicrotubule chemotherapy agents, Annu. Rev. Med. 48 (1997) 353–374. https://doi:10.1146/annurev.med.48.1.353.
[44] A. Rabzia, M. Khazaei, Z. Rashidi, M.R. Khazaei, Synergistic anticancer effect of paclitaxel and noscapine on human prostate cancer cell lines, Iran. J. Pharm. Res. (IJPR) 16 (4) (2017) 1432–1442.
[45] D. Muthiah, G.K. Henshaw, A.J. DeBono, B. Capuano, P.J. Scammells, R. Callaghan, Overcoming P-Glycoprotein-Mediated drug resistance with noscapine derivatives, Drug Metab. Dispos. 47 (2) (2019 Feb) 164–172, https://doi.org/10.1124/dmd.118.083188. Epub 2018 Nov 26. PMID: 30478158.
[46] P.M. Checchi, J.H. Nettles, J. Zhou, J.P. Snyder, H.C. Joshi, Microtubule-interacting drugs for cancer treatment, Trends Pharmacol. Sci. 24 (7) (2003 Jul) 361–365, https://doi.org/10.1016/S0165-6147(03)00161-5. PMID: 12871669.